

# The Pomeron intercept in $\lambda\phi^3$ theory in 4 Minkowski + 1 compact dimensions

**K. Tuchin\***

*HEP Department  
School of Physics and Astronomy,  
Raymond and Beverly Sackler Faculty of Exact Science,  
Tel-Aviv University, Ramat Aviv, 69978, Israel*

July, 2000

## **Abstract**

We calculate the total cross section for two scalar particles scattering at high energies in  $\lambda\phi^3$  theory in five dimensions, four of which are usual Minkowski ones and the fifth is compact. It is shown that the cross section is dominated by exchange of Pomeron whose intercept is larger than in usual four-dimensional case.

# 1 Introduction

The total cross section for various hadron interactions at high energy is dominated by the exchange of the Pomeron. The Pomeron is defined as a Reggeon (a pole in the scattering amplitude) with intercept close to unity. This definition implies the following scaling of the total cross section with energy:

$$\sigma_{tot} = \sigma_0 \left( \frac{s}{s_0} \right)^\Delta, \quad (1)$$

where  $s$  is the center-of-mass energy squared,  $\sigma_0$  and  $s_0$  are certain constants[1, 2].  $1 + \Delta$  is called the Pomeron intercept. Experimental data can be fitted well with the value  $\Delta = 0.08$ [3].

In QCD, high energy (leading logarithmic) behaviour of the scattering amplitude is described by the solution of the BFKL equation[4]. It exhibits Pomeron-like behaviour of Eq. (1) with  $\Delta = 4 \ln 2 \alpha_s N_c / \pi$ . However, there are several problems with this solution. First, numerically this value is much larger than experimentally observed one. Second, the leading singularity of the scattering amplitude is a cut rather than pole, so that actually, the asymptotic behaviour of  $\sigma_{tot}$  is more complicated than that of Eq. (1). Third, the next-to-leading order corrections to this solution are so large that they threaten to spoil the perturbative approach[5]. Several authors suggested how to cure this discrepancy (see Ref. [6] for a brief review). In addition, it was shown in Ref. [7] that the non-perturbative QCD effects could be responsible for the appearance of the Pomeron pole (instead of the BFKL cut) in the scattering amplitude.

In this note we will not be concerned with those problems, rather we will show that the Pomeron intercept obtains corrections of completely different origin.

In recent years the interest arose in theories of Kaluza-Klein type in which extra compact dimensions are introduced in order to incorporate gravity into quantum field theory. The 4-dimensional field theory can be thought of as a low-energy effective theory of graviton excitations and their interactions with matter. If the radius of compactification is  $R$ , then at energies  $s > 1/R^2$  certain observables will show dependence on the scale  $R$ . It was even argued in the framework of the string theory, that effects of quantum gravity could be seen at energies on the order of 1 TeV which will be accessible at LHC[8]. The theories of that kind investigate impact of gravity on the elementary particles physics. On the contrary we will assume that the gravity is completely negligible at the energy scale we are interested in. If any compact dimensions exist they will manifest themselves as a corrections to the processes at high energies even in the flat space-time. We will sum up all such corrections for one particular process and show that this leads to increase of the Pomeron intercept.

In this letter we discuss a simple model of the Pomeron[9]. This model is based on a scalar theory with cubic self-interactions. Despite its simplicity this model shows many features of the more realistic QCD Pomeron[1, 2]. In particular, the Pomeron of  $\lambda\phi^3$  corresponds to the leading pole in the scattering amplitude as we expect from non-perturbative QCD calculations[7].

## 2 Calculation of the total cross section

Suppose, for simplicity, that there exist only one compact dimension of radius  $R$ . Let us determine what are the corrections to the Pomeron of the 4-dimensional  $\lambda\phi^3$  theory which stem from this assumption. To this end we are going to calculate the high energy asymptotic of the total cross section for the two scalar particles scattering.

The  $\lambda\phi^3$  theory in 5-dim is defined by the following action:

$$S = \int d^4x \int_0^{2\pi R} dy \left( \frac{1}{2} \partial_M \Phi(x, y) \partial^M \Phi(x, y) - \frac{\lambda_5}{3!} \Phi^3 \right) , \quad (2)$$

where  $x^\mu$  are the usual four dimensional space-time coordinates of Minkowski space and  $y$  is a space coordinate of the compact fifth dimension.  $\Phi(x, y)$  is a self-coupled scalar field,  $\lambda_5$  is a coupling constant.  $M = 0, 1, 2, 3, 4$ ,  $\mu = 0, 1, 2, 3$ . The metric is flat with signature  $\{1, -1, -1, -1, -1\}$ . Imposing untwisted boundary condition on the scalar field,  $\Phi(x, y + 2\pi R) = \Phi(x, y)$  one can expand  $\Phi$  in a Fourier series

$$\Phi(x, y) = \frac{1}{\sqrt{2\pi R}} \sum_{n=-\infty}^{\infty} \phi_n(x) e^{in\frac{y}{R}} = \frac{1}{\sqrt{2\pi R}} \left[ \phi_0(x) + 2 \sum_{n=1}^{\infty} \phi_n(x) \cos \frac{ny}{R} \right] \quad (3)$$

where we used the fact that  $\Phi$  is hermitian operator implying  $\phi_{-n} = \phi_n$ .

In order to see how the corrections appear, it is convenient to perform calculations in 4-dimensional effective theory. Upon substitution of Eq. (3) into Eq. (2) and integration over  $y$  we obtain the effective 4-dimensional action which reads<sup>1</sup>

$$S = \int d^4x \left\{ \frac{1}{2} (\partial_\mu \phi_0)^2 - \frac{\lambda_4}{3!} \phi_0^3 + \sum_{n=1}^{\infty} (\partial_\mu \phi_n)^2 - \frac{1}{2} \sum_{n=1}^{\infty} \frac{2n^2}{R^2} \phi_n^2 - 2 \frac{\lambda_4}{2!} \phi_0 \sum_{n=1}^{\infty} \phi_n^2 - \frac{\lambda_4}{3!} 6 \sum_{m,n=1}^{\infty} \phi_n \phi_m \phi_{m+n} \right\} , \quad (4)$$

where we have defined  $\lambda_4 = \lambda_5 / \sqrt{2\pi R}$ . The Feynman rules associated with this theory are shown in Fig. 1. Note, that the field  $\phi_0$  corresponds to usual 4-dimensional theory, while  $\phi_n$  are excitations with masses  $m_n^2 = 2n^2/R^2$ . Since  $\phi_0$  is massless it the only field that survives in the low energy limit  $s \ll 1/R^2$ .

The dominant contribution to the total cross section for  $\phi_0\phi_0$  scattering in the leading logarithmic approximation (LLA) ( $\alpha \ll 1$ ,  $\alpha \log s \sim 1$ ) arises from the ladder diagrams[1, 2] In the Fig. 2 some diagrams contributing to the order  $\alpha^6$  (four rungs) are shown ( $\alpha = \lambda^2/4\pi$ ). We subdivide all ladders at any order of  $\alpha$  (fixed number of rungs  $r$ ) into four kinds.

1. First, there is the unique ladder without dashes lines (Fig. 2a). This is the only diagram which contributes in the usual 4-dimensional  $\lambda\phi^3$  theory.
2. Second, there are diagrams with *separate simple* dashed loops, i.e. without any two dashed loops having common rung; any simple loop includes only two neighbor rungs by definition. (Fig. 2b).

---

<sup>1</sup>The following elementary integrals for integer numbers  $n, m, p \geq 1$  where used:

$$\begin{aligned} \int_0^{2\pi R} dy \cos \frac{ny}{R} &= 0 , \\ \int_0^{2\pi R} dy \cos \frac{ny}{R} \cos \frac{my}{R} \cos \frac{py}{R} &= \frac{\pi}{2} R (\delta_{n,m+p} + \delta_{m,n+p} + \delta_{p,m+n}) , \\ \int_0^{2\pi R} dy \cos \frac{ny}{R} \cos \frac{my}{R} &= \pi R \delta_{m,n} , \end{aligned}$$

and the same are for sin.

3. Third, there are diagrams which contain at least one pair of *merged* simple dashed loops (Fig. 2c).

4. Fourth, all other diagrams (Fig. 2d).

Let us calculate the contribution of the  $r$ -rung diagram of the first kind. Our notations are defined in Fig. 3. Using optical theorem and Landau-Cutkosky cutting rules we get

$$\begin{aligned} \sigma^r(1^{\text{st}}) &= \frac{2}{s} \prod_{i=1}^{r+1} \left( \int \frac{d^4 k_i}{(2\pi)^4} \right) \lambda^2 \prod_{i=1}^{r+1} \left( \frac{\lambda^2}{k_i^4} \right) \\ &\quad \times 2\pi\delta\left((p_1 - k_1)^2\right) \prod_{i=1}^r \left( 2\pi\delta\left((k_i - k_{i+1})^2\right) \right) 2\pi\delta\left((p_2 + k_{r+1})^2\right) \end{aligned} \quad (5)$$

It is convenient to introduce the Sudakov variables:

$$\begin{aligned} k_i &= \alpha_i p_1 + \beta_i p_2 + k_{i\perp} \quad , \\ d^4 k_i &= \frac{s}{2} d\alpha_i d\beta_i d^2 k_{i\perp} \quad , i = 1, \dots, r+1 \end{aligned}$$

Leading log  $s$  approximation stems from the following kinematical region

$$\alpha_{r+1} \ll \alpha_r \ll \dots \ll \alpha_1 \ll 1 \quad , \quad \beta_1 \ll \beta_2 \ll \dots \ll \beta_{r+1} \ll 1 \quad .$$

Performing integrations in Eq. (5) in this kinematical region yields

$$\sigma^r(1^{\text{st}}) = 16\pi^2 \alpha \Sigma \frac{1}{s^2} \Sigma^r \frac{1}{r!} \ln^r \frac{s}{q^2} \quad , \quad (6)$$

where  $q$  is a typical transverse momentum,

$$\Sigma = \alpha \int \frac{d^2 k_{\perp}}{(2\pi)^2} \frac{1}{k_{\perp}^4} = \frac{\alpha}{4\pi\mu^2} \quad (7)$$

and  $\mu$  is infrared cutoff. Since the integral over  $k_{\perp}$  converges at large  $k_{\perp}$  as  $1/k_{\perp}^2$  we set the upper limit of the integration to be infinity.

The diagrams of the second kind with given number of rungs can be drawn by taking the diagram of the first kind and replacing solid loops by dashed ones in such a way that all dashed loops are simple and separate. This replacement means, that

- every propagator corresponding to the cut dashed line ( $t$ -channel one) becomes  $2\pi\delta(k^2 - 2n^2/R^2)$ . However, in LLA kinematics contribution of the massless  $t$ -channel propagators is the same as the massive ones. Thus, integration over the longitudinal Sudakov variables  $\alpha_i$  and  $\beta_i$  yields the same contribution  $\frac{1}{r!} \ln^r s$  as in Eq. (6). Assume, that the integration over delta functions is done. Then,
- the remaining integration over every dashed loop is performed over the transverse momentum which replaces the corresponding solid loop contribution as follows<sup>2</sup>:

$$\Sigma = \alpha \int \frac{d^2 k_{\perp}}{(2\pi)^2} \frac{1}{k_{\perp}^4} = \frac{\alpha}{4\pi\mu^2} \longrightarrow 2^4 \alpha \sum_{n=1}^{\infty} \int \frac{d^2 k_{\perp}}{(2\pi)^2} \frac{1}{\left(|k_{\perp}^2| + \frac{2n^2}{R^2}\right)^2} = \frac{\alpha \pi R^2}{3} \quad , \quad (8)$$

---

<sup>2</sup>Recall that  $k_{\perp}$  is a space-like 4-vector

The factor  $2^4$  arises from the  $\phi_0\phi_n^2$  vertex, the coupling of which is twice as big as  $\phi_0^3$  one (see Fig. 1). This equation implies that every pair of  $s$ -channel propagators gives contribution of the order  $\mathcal{O}(R^2)$  to the cross section. In general, one can introduce the simple dashed loop into the  $r$ -rung diagram of the first kind in  $C_{r+1}^1 = r + 1$  ways<sup>3</sup>. Further, there are  $C_{r+1}^k$  ways to insert  $k$  simple dashed loops into the  $r$ -rung ladder of the first kind. It is easy to verify that from those there are only<sup>4</sup>

$$C_{r+1}^k - \sum_{l=1}^{k-1} C_{r-l+1}^{k-l} = C_{r+1}^k - C_{r+1}^{k-1} + 1 \quad (9)$$

ways to get the ladder of the second kind ( $k \geq 1, r \geq 0$ ).

Next, concentrate on ladders with only simple dashed loops (Fig. 2b,c) or without them (Fig. 2a). The number of diagrams of different kinds contributing to the  $r$ -rung ladder is given by

$$\begin{aligned} & 1 \quad , \quad \text{of 1st kind} \\ & \sum_{k=1}^{\frac{\tilde{r}}{2}+1} (C_{r+1}^k - C_{r+1}^{k-1} + 1) \quad , \quad \text{of 2nd kind} \end{aligned} \quad (10)$$

$$\sum_{k=\frac{\tilde{r}}{2}+2}^{r+1} C_{r+1}^k + \sum_{k=1}^{\frac{\tilde{r}}{2}+1} (C_{r+1}^{k-1} - 1) \quad , \quad \text{of 3rd kind} \quad (11)$$

$$\sum_{k=0}^{r+1} C_{r+1}^k = 2^{r+1} \quad , \quad \text{altogether} \quad (12)$$

where  $\tilde{r} = \begin{cases} r & , \quad r \text{ even,} \\ r-1 & , \quad r \text{ odd.} \end{cases}$

We will demonstrate now, that the calculation can be significantly simplified in the LLA. Consider for example, contribution of the first and second kind of diagrams. Using Eq. (10) and Eq. (8) in Eq. (6) yields

$$\sigma(1^{\text{st}} + 2^{\text{nd}}) = \frac{4\pi\alpha^2}{s^2\mu^2} \left\{ \sum_{r=0}^{\infty} \frac{1}{r!} \ln^r \frac{s}{q^2} \left( \frac{\alpha}{4\pi\mu^2} \right)^r \left[ 1 + \sum_{k=1}^{\frac{\tilde{r}}{2}+1} \left( \frac{4\mu^2\pi^2 R^2}{3} \right)^k (C_{r+1}^k - C_{r+1}^{k-1} + 1) \right] \right\} \quad (13)$$

Instead of summing over  $\sum_{r=0}^{\infty} \sum_{k=1}^{\frac{\tilde{r}}{2}+1}$  it is convenient to sum in a different order  $\sum_{k=1}^{\infty} \sum_{\tilde{r}=2k-2}^{\infty}$  i.e. we want to sum all contributions to the given order  $\mathcal{O}(R^{2k})$  first. The key observation is that in the LLA the following equation holds

$$\sum_{r=j}^{\infty} \frac{1}{r!} \ln^r \frac{s}{q^2} a^r r^n \approx \left( \frac{s}{q^2} \right)^a a^n \ln^n \frac{s}{q^2} \quad , \quad (14)$$

for any integers  $0 \leq j, n < \infty$ . This means that the combinatorial factor in Eq. (13) reads

$$C_{r+1}^k - C_{r+1}^{k-1} + 1 \approx C_r^k \quad . \quad (15)$$

<sup>3</sup> $C_j^i = \frac{j!}{i!(j-i)!}$ .

<sup>4</sup>Note the following relation  $\sum_{l=1}^{k-1} C_{r-l+1}^{k-l} = C_{r+1}^{k-1} - 1$ .

In particular, the contribution of the ladders of the third and fourth kinds is negligible. Indeed, consider Eq. (11). Using the symmetry of binomial coefficients  $C_r^k = C_r^{r-k}$  it is easy to rewrite the left hand term in Eq. (11) as follows:

$$\sum_{k=\frac{\tilde{r}}{2}+2}^{r+1} C_{r+1}^k = \sum_{k'=1}^{r-\frac{\tilde{r}}{2}} C_{r+1}^{r-\frac{\tilde{r}}{2}-k'}. \quad (16)$$

The number of diagrams of the fourth kind (Fig. 2d) is equal to that given in Eq. (11) multiplied by a certain function of the number  $k$ . From Eqs. 10,11,15 and 16 we see that the total contribution of the third and fourth kind ladders is negligible in comparison with that of the first and second kinds at any order  $\mathcal{O}(R^{2k})$ . This result justifies our classification of ladder diagrams.

Using Eq. (15) in Eq. (13) and summing over  $r$  and  $k$  we obtain the total cross section in the LLA. It reads

$$\sigma = \frac{4\pi\alpha^2}{s^2\mu^2} \left( \frac{s}{q^2} \right)^{\frac{\alpha}{4\pi\mu^2} \left( 1 + \frac{4\pi^2\mu^2 R^2}{3} \right)}. \quad (17)$$

We thus see, that the 5-dimensional Pomeron intercept equals

$$1 + \Delta_{5\text{dim}} = 1 + \underbrace{\frac{\alpha}{4\pi\mu^2}}_{\Delta_{4\text{dim}}} \left( 1 + \frac{4\pi^2\mu^2 R^2}{3} \right) \quad (18)$$

i.e. it gets the positive contribution at energies  $s > 1/R^2$  as compared to the 4-dimensional one.

Our general result, that the fifth space-like compact dimension increases the value of the Pomeron intercept, is valid in the QCD case as well. The positiveness is assured by the integration analogous to that in Eq. (8). Since the QCD coupling is dimensionless (in 4 dimensions) correction to the Pomeron intercept is of the order  $\sim +\alpha_S R^2 m_\pi^2$ . So, the QCD Pomeron intercept is equal to  $1 + \Delta_{4\text{dim}} + c\alpha_S R^2 m_\pi^2$ , where  $c$  is a certain unknown constant, while  $\Delta_{4\text{dim}}$  arises from 4-dimensional theory[4, 5, 7]. Thus, had we known the value  $\Delta_{4\text{dim}}$ , we would have estimated the size of extra dimension  $R$ . Meanwile we are used to think that there are no manifestations of extra dimensions at accesible energies, i.e.  $R^2 m_\pi^2 \ll 1$  in QCD.

To conclude, we studied the influence of the fifth compact dimension on the Pomeron intercept in  $\lambda\phi^3$  theory and found that it gets positive correction which is proportional to the squared radius of the compact dimension. We expect that the same qualitative behavior is valid in QCD. This result has impact on both the study of high energy behaviour of the scattering amplitude and search of phenomenological signatures of extra dimensions.

**Acknowledgments.** I wish to thank Professor E. Levin for numerous helpful discussions and comments as well as for reading the manuscript and providing me with many refernces. I would like to acknowledge an interesting discussions with S. Bondarenko, Yu. Kovchegov and Ed. Sarkisyan.

## References

- [1] E. Levin, *Everything about reggeons*, hep-ph/9710546, TAUP 2465-97, DESY 97-213; P.D.B. Collins, *An introduction to Regge theory and High energy physics*, Cambridge U.P., 1977.
- [2] J.R. Forshaw and D.A. Ross, *Quantum Chromodynamics and the Pomeron*, Cambridge University Press, 1997.
- [3] A. Donnachie and P.V. Landshoff, *Nucl. Phys.* **B244**:322 (1984), *Nucl. Phys.* **B267**:690 (1986), *Phys. Lett.* **B296**:227 (1992), *Z. Phys.* **C61**:139 (1999).
- [4] L.N. Lipatov, *Sov. J. Nucl. Phys.* **23**:338 (1976), E.A. Kuraev, L.N. Lipatov and V.S. Fadin, *Sov. Phys. JETP* **44**:443 (1976); *Sov. Phys. JETP* **45**:199 (1977); Ya. Balitskii and L.N. Lipatov, *Sov. J. Nucl. Phys.* **28**:822 (1978).
- [5] V.S. Fadin and L.N. Lipatov, *Phys. Lett.* **B429**:127 (1998); M. Ciafaloni and G. Camici, *Phys. Lett.* **B430**:349 (1998), and references therein.
- [6] G.P. Salam, hep-ph/0005304, and references therein.
- [7] D. Kharzeev and E. Levin, *Nucl. Phys.* **B578**:351 (2000); D. Kharzeev, Yu. Kovchegov and E. Levin, hep-ph/0007182, BNL-NT-00/18, TAUP-2637-2000.
- [8] G.F. Giudice, R. Rattazi and J.D. Wells, *Nucl. Phys.* **B544**:3 (1999), and references therein.
- [9] D.A. Amati, S. Fubini and A. Stanghellini, *Nuovo Cim.* **26**:896 (1962). The collection of the best original papers on Reggeon approach can be found in *Regge Theory of low  $p_t$  Hadronic Interactions*, ed. L. Caneschi, North-Holland, 1989.

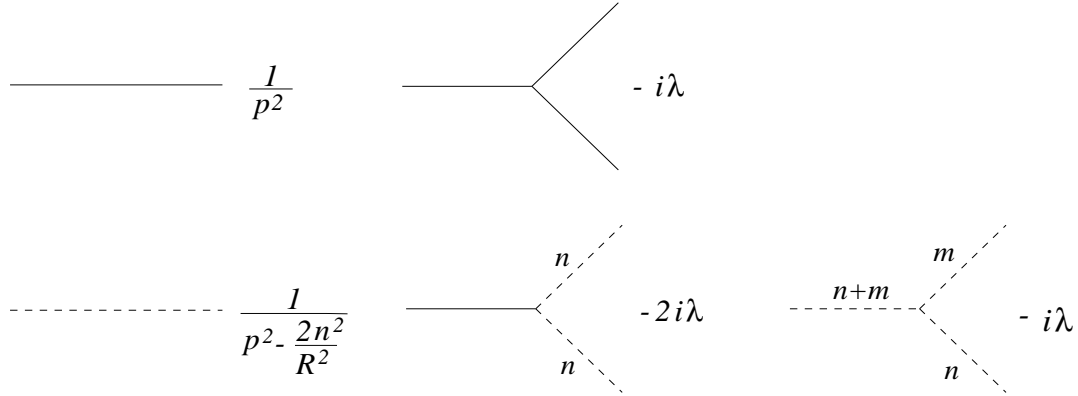


Figure 1: *The Feynman rules for the action Eq. (4). Solid lines correspond the massless scalar field  $\phi_0$ , dashed lines – to massive scalar fields  $\phi_n$ . The amplitude must be summed over any free indecies  $n$ ,  $n \geq 1$ .*

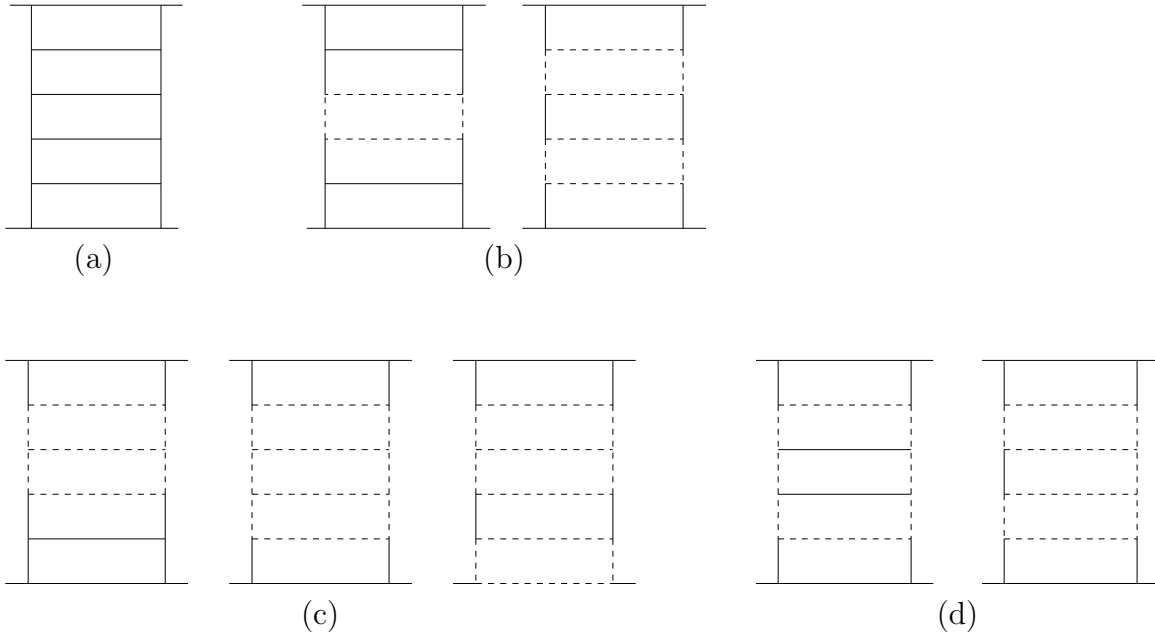


Figure 2: *Some ladder diagrams of the order  $\alpha^6$ . (a) The ladder of the first kind: no dashed lines appear, (b) ladders of the second kind: only simple separate dashed loops appear, (c) ladders of the third kind: there are merged simple dashed loops and (d) ladders of the fourth kind. Note, that one can get ladders of the kind (d) by replacing the dashed lines inside merged dashed loops in diagrams of type (c) by the solid ones.*



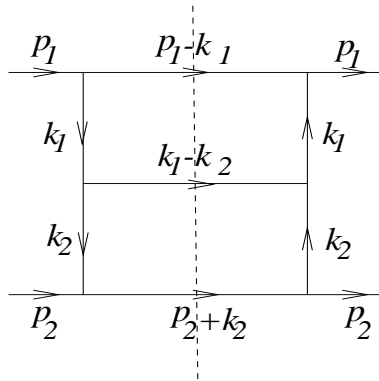


Figure 3: *Notations for the one rung ladder diagram. Generalization for arbitrary  $r$  is straightforward. Dashed line is a  $t$ -channel cut.*